Chemistry of Phosphine – Borane Adducts at Platinum Centers: Synthesis and Reactivity of Pt^{II} Complexes with Phosphinoborane Ligands

Cory A. Jaska,[a] Hendrik Dorn,[a,b] Alan J. Lough,[a] and Ian Manners*[a]

Abstract: Reaction of $[Pt(PEt_3)_3]$ with the primary and secondary phosphine – borane adducts $PhRPH \cdot BH_3$ (R = H, Ph) resulted in oxidative addition of a P–H bond at the Pt^0 center to afford the complexes *trans*-$[PtH(PPhR \cdot BH_3)(PEt_3)_2]$ (**1**: R = H; **2**: R = Ph). The products **1** and **2** were characterized by ^1H, ^{11}B, ^{13}C, ^{31}P, and ^{195}Pt NMR spectroscopy, and the molecular structures were verified by X-ray crystallography. In both cases, a *trans* arrangement of the hydride ligand with respect to the phosphidoborane ligand was observed. When **2** was treated with $PhPH_2 \cdot BH_3$, a novel phosphidoborane ligand-exchange reaction occurred which yielded **1** and $Ph_2PH \cdot BH_3$. Treatment of **2** with one equivalent of depe (depe = 1,2-bis(diethylphosphino)ethane) resulted in the formation of the complex *cis*-$[PtH(PPh_2 \cdot BH_3)(depe)]$ (**3**), in which the hydride ligand and the phosphidoborane ligand are in a *cis* arrangement. Treatment of **3** with $PhPH_2 \cdot BH_3$ was found to result in an exchange of the phosphidoborane ligands to give the complex *cis*-$[PtH(PPhH \cdot BH_3)(depe)]$ (**4**) and $Ph_2PH \cdot BH_3$. Complex **4** was found to undergo further reaction in the presence of $PhPH_2 \cdot BH_3$ to give *meso*-*cis*-$[Pt(PPhH \cdot BH_3)_2(depe)]$ (**5**) and *rac*-*cis*-$[Pt(PPhH \cdot BH_3)_2(depe)]$ (**6**).

Keywords: boranes · dehydrocoupling · hydrides · P ligands · platinum

Introduction

Metal-catalyzed reactions have had an enormous impact in the area of organic synthesis, whereas the application of transition metal catalysis to the formation of homonuclear or heteronuclear bonds between inorganic elements is relatively unexplored. Facile and convenient catalytic coupling reactions would be key advances in inorganic synthetic methodology and would function as important alternatives to classical reactions, such as salt metathesis. The discovery of catalytic dehydrocoupling routes to Si–Si bonds in the mid 1980's[1] and the application of this methodology to the synthesis of polysilanes $[SiRR']_n$ generated considerable interest in the development of new synthetic methods to produce rings, chains, and macromolecules based on main-group elements.[2] Subsequently, transition metal-catalyzed dehydropolymerization routes to polygermanes[3, 4] $[GeRR']_n$ and polystannanes[5] $[SnRR']_n$ have been described and the dehydrocoupling methodology has also been extended to include reactions which form new P–P,[6] B–Si,[7] Si–P,[8] Si–N[9] Si–C,[10] Sn–Te[11] and Si–O[12] bonds. Recently, we have reported a novel catalytic route towards P–B bond formation that involves the dehydrocoupling of primary or secondary phosphine – borane adducts in the presence of late transition-metal catalysts to afford linear and cyclic oligomeric species as well as high molecular weight polyphosphinoboranes [Eq. (1) – (3)].[13–17]

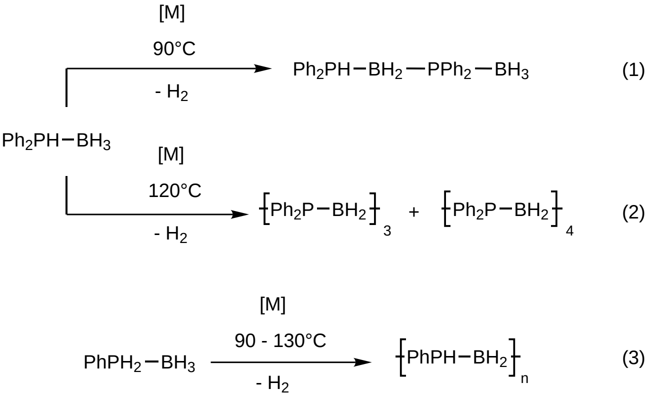

[M] = Transition Metal Catalyst

As part of our ongoing research into the synthesis and properties of polymers based on a backbone of alternating four-coordinate phosphorus and boron atoms, an understanding of the dehydropolymerization mechanism is of consid-

---

[a] Prof. I. Manners, C. A. Jaska, Dr. H. Dorn, Dr. A. J. Lough
Department of Chemistry, University of Toronto
80 St. George Street, Toronto, ON, M5S 3H6 (Canada)
Fax: (+1)416-978-2450
E-mail: imanners@chem.utoronto.ca

[b] Prof. I. Manners
Current Address: Ontario Centre of Forensic Sciences
25 Grosvenor Street, Toronto, ON, M7A 2G8 (Canada)

erable fundamental interest. This knowledge might allow for the development of more efficient catalysts that could effectively lower the required temperature and allow access to higher molecular weight polymers (>30000). Late transition-metal complexes that operate as dehydropolymerization catalysts are quite rare,[5c, 6c, 12, 18, 19] and detailed investigations into the mechanisms of the corresponding catalytic cycles have yet to appear in the literature. In contrast, the dehydropolymerization of silanes and stannanes with Group 4 metallocene complexes has been extensively investigated and has resulted in the development of more efficient catalysts.

A plausible first step in the catalytic dehydrocoupling of phosphine–borane adducts may involve insertion of the transition metal into either the P–H or B–H bond, followed by subsequent σ-bond metathesis and/or oxidative addition/reductive elimination steps. Previous studies of late transition metal-catalyzed hydroboration and hydrophosphination reactions have supplied ample precedents for insertion of late transition metals into both P–H and B–H bonds. For example, the oxidative addition of P–H bonds of phosphines and phosphine oxides at Pt^0 or Pd^0 centers has been reported and is believed to be a key step in the catalytic hydrophosphination of alkenes and alkynes.[20] In some cases, potential intermediate species in the catalytic cycle that contain Pt or Pd hydrides have been isolated and structurally characterized.[21] Insertion of Rh^I and Ir^I centers[22] into B–H bonds to afford metal boryl complexes has also been demonstrated.[23] More recently, reactions involving $Me_3P\cdot BH_3$ and $Me_3P\cdot BH_2BH_2\cdot PMe_3$ have resulted in B–H bond activation and led to structurally characterized examples of mononuclear and dinuclear metal boryl complexes.[24] In addition, σ-borane[25] complexes and η^1-borane[26] complexes have also been reported.

However, there has been no investigation into the oxidative-addition chemistry involving late transition-metal compounds with phosphine–borane adducts that contain both P–H and B–H bonds. Thus, to fully investigate the potential mechanistic pathways that may operate during the transition-metal-catalyzed P–B bond-formation process, a study of the coordination chemistry of the adducts bearing both P–H and B–H bonds is desirable. In this paper,[27] we report full details of our studies on the reactions of $Ph_2PH\cdot BH_3$ and $PhPH_2\cdot BH_3$ with the Pt^0 species $[Pt(PEt_3)_3]$, and include a reactivity study of the resultant complexes.

Results and Discussion

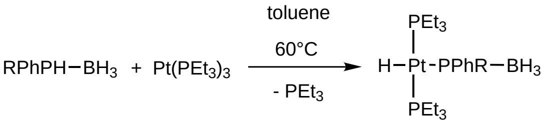

$$RPhPH{-}BH_3 + Pt(PEt_3)_3 \xrightarrow[-\,PEt_3]{\text{toluene, }60^\circ C} H{-}Pt(PEt_3)_2{-}PPhR{-}BH_3 \qquad (4)$$

1: R = H
2: R = Ph

Formation of *trans*-$[PtH(PPhR\cdot BH_3)(PEt_3)_2]$ (1: R = H; 2: R = Ph): To investigate the potential oxidative-addition chemistry of phosphine–borane adducts bearing both P–H and B–H bonds with transition metal centers, the primary and secondary adducts $PhRPH\cdot BH_3$ (R = H, Ph) were reacted with $[Pt(PEt_3)_3]$ at 60 °C in toluene. Insertion of the Pt center into the P–H bond was observed with the formation of the complexes *trans*-$[PtH(PPhR\cdot BH_3)(PEt_3)_2]$ (**1**: R = H; **2**: R = Ph; [Eq. (4)]). Upon workup and recrystallization from hexanes, the yields of isolated products for the yellow-orange complexes **1** and **2** were found to be 23 % and 63 %, respectively. The low yield for **1** may be caused by the decomposition of the complex when heated for prolonged periods of time at 60 °C. Unfortunately, the insertion reaction that produces **1** is much more sluggish than that for complex **2** and requires a longer reaction time (21 h); this may contribute significantly to the low yields observed. Complex **1** was fully characterized by ^1H, ^{11}B, ^{13}C, ^{31}P, and ^{195}Pt NMR spectroscopy, mass spectrometry, IR spectroscopy, and by X-ray crystallography. The spectroscopic evidence obtained was indicative of the insertion of a $[Pt(PEt_3)_2]$ fragment into the P–H bond of the phosphine–borane adduct, rather than insertion into the B–H bond. For example, the ^1H-coupled ^{31}P NMR spectrum of **1** showed two sets of signals: 1) a doublet at $\delta = 17.9$ ppm, which is assigned to the PEt_3 ligands attached to Pt that show coupling to one other phosphorus nucleus ($^2J(P,P) = 19$ Hz) as well as ^{195}Pt satellites ($^1J(P,Pt) = 2572$ Hz), and 2) a broad doublet of quartets at $\delta = -48.7$ assigned to the $PPhH\cdot BH_3$ moiety, which arises from coupling with the quadrupolar boron nucleus (for ^{11}B, $I = 3/2$, $^1J(P,B) \approx 55$ Hz) and one adjacent hydrogen substituent ($^1J(P,H) = 299$ Hz), in addition to ^{195}Pt satellites ($^1J(P,Pt) = 1440$ Hz) (Figure 1 a). The ^{11}B NMR spectrum showed a single broad resonance at $\delta = -33.2$, which is in a region typical for resonances of BH_3 adducts of phosphines. The spectrum did not display any coupling to the phosphorus nucleus, while the ^1H-coupled spectrum did not show any distinguishable coupling to the three hydride protons; rather it resulted in a broadening of the signal. The ^1H NMR spectrum showed the presence of phenyl and ethyl groups, as well as a broad doublet at $\delta = 4.39$ ($^1J(H,P) = 299$ Hz) assigned to the P-H proton of the phosphidoborane ligand. The hydridic B-H protons, which typically occur as a broad 1:1:1:1 quartet, were obscured by the signals for the ethyl groups. The key feature of the ^1H NMR spectrum was the low-frequency hydride resonance signal at $\delta = -5.74$ ppm, which appeared as a doublet of triplets with a larger coupling to one phosphorus nucleus ($^2J(H,P) = 125$ Hz) and a smaller coupling to two phosphorus nuclei ($^2J(H,P) = 15$ Hz) as well as ^{195}Pt satellites ($^1J(H,Pt) = 872$ Hz) (Figure 1 b). The ^{195}Pt NMR spectrum displayed a triplet of doublets of doublets at $\delta = -3541$ ppm (Figure 1 c). This pattern arises from coupling to the two equivalent PEt_3 ligands ($^1J(Pt,P) = 2573$ Hz) as well as coupling to the phosphorus of the phosphine-borane ligand ($^1J(Pt,P) = 1462$ Hz) and the hydride ligand ($^1J(Pt,H) = 820$ Hz). The NMR evidence was consistent with the presence of one substituent ($PPhH\cdot BH_3$) *trans* and two equivalent substituents (PEt_3) *cis* to the hydride ligand. The EI mass spectrum showed a peak at *m*/*z* 541, corresponding to the loss of a BH_3 group from the parent molecular ion. This type of loss is a typical feature for phosphine–borane adducts synthesized in

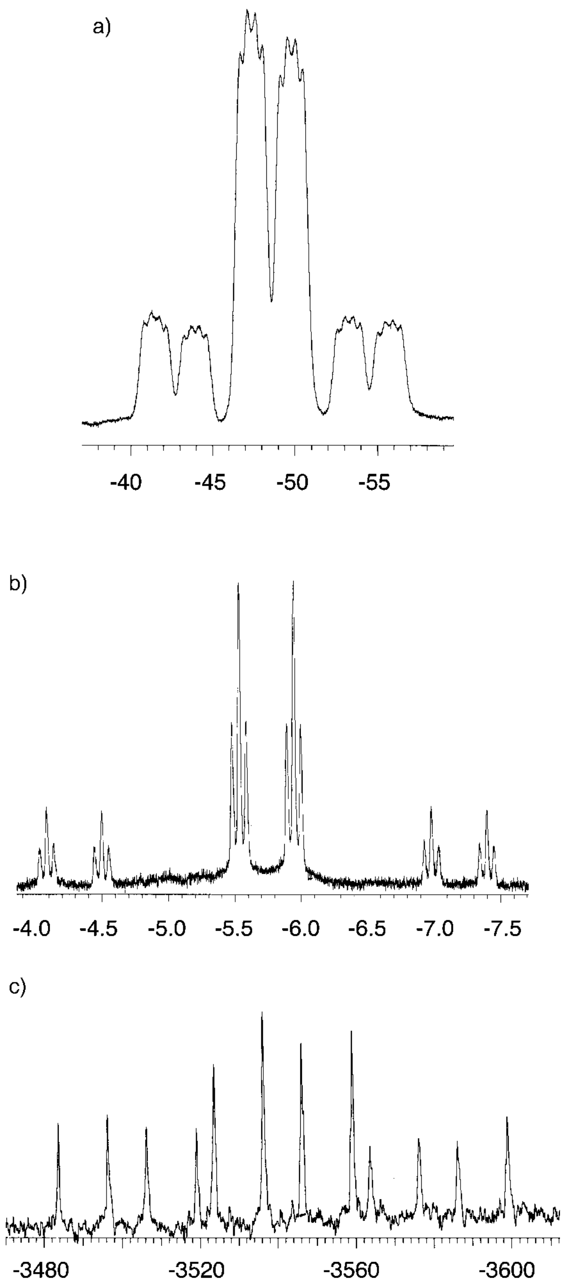

Figure 1. NMR spectra of *trans*-[PtH(PPhH · BH_3)(PEt_3)$_2$] (**1**). a) ^{31}P NMR (PPhH–BH_3 region) (^1J(H,P) = 299 Hz, ^1J(B,P) ≈ 55 Hz, ^1J(Pt,P) = 1440 Hz). b) ^{1}H NMR (hydride region) (^2J(H,P_{cis}) = 15 Hz, ^2J(H,P_{trans}) = 125 Hz, ^1J(Pt,H) = 872 Hz). c) ^{195}Pt NMR (^1J(Pt,P) = 2573 Hz, ^1J(Pt,P) = 1462 Hz, ^1J(Pt,H) = 820 Hz).

our group and is indicative of the relative weakness of the donor–acceptor nature of the P–B interaction. The IR spectrum of **1**, taken as a Nujol mull between KBr plates, shows two medium intensity bands at $\tilde{\nu}$ = 2350 and 2022 cm^{-1}, which correspond to B–H and Pt–H stretches, respectively.

Full spectroscopic characterization was also performed for complex **2**, many features of which are similar in nature to those seen for **1**. For example, two signals in the ^{31}P{^{1}H} NMR spectrum were observed at δ = 16.7 (PEt_3) and −3.7 ppm ($PPh_2 \cdot BH_3$) along with their ^{195}Pt satellites, while the ^{11}B NMR spectrum showed a broad signal at δ = −31.4 ppm. Again, the most convincing evidence for a *trans* arrangement appeared in the hydride region of the ^{1}H NMR spectrum, which displayed a doublet of triplets at δ = −6.75 ppm, flanked by ^{195}Pt satellites. This coupling pattern is characteristic of the hydride ligand coupling with one phosphorus nucleus *trans* and two equivalent phosphorus nuclei *cis*, as seen in the case of **1**. The ^{195}Pt NMR spectrum showed a signal at δ = −3450 ppm with a tdd coupling pattern and approximately the same Pt–P and Pt–H coupling constants as those observed in the ^{1}H and ^{31}P NMR spectra. The mass spectrum of **2** again shows loss of a BH_3 group as the highest *m*/*z* peak (617), while the IR spectrum shows B–H and Pt–H stretches at $\tilde{\nu}$ = 2341 and 2009 cm^{-1}, respectively.

X-ray crystallographic analysis of 1 and 2: To confirm the assigned molecular structures of **1** and **2**, single-crystal X-ray analyses were performed. They were found to be consistent with the spectroscopic data obtained. The molecular structure of **1** is shown in Figure 2, bond lengths and angles are given in Table 1. The geometry around the Pt^{II} center is distorted square-planar with *trans* PEt_3 ligands. Unfortunately, it was not possible to find and resolve the hydride proton during the X-ray study; however, its presence can be inferred from the rather large P(3)-Pt(1)-P(2) angle of 168.26(5)°, in addition to the previously mentioned ^{1}H NMR data. The lengths of

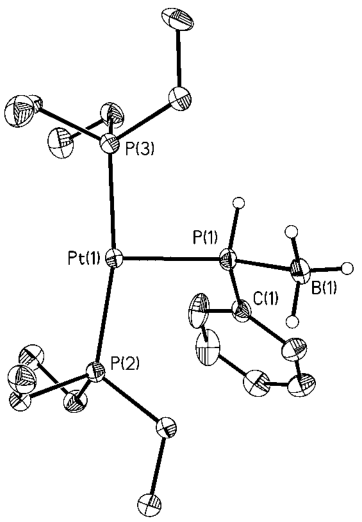

Figure 2. Molecular structure of *trans*-[PtH(PPhH · BH_3)(PEt_3)$_2$] (**1**). All hydrogen atoms bonded to carbon are omitted for clarity. Selected bond lengths and angles are presented in Table 1.

Table 1. Selected bond lengths [Å] and angles [°] for **1**.

Pt(1)–P(1)	2.3477(14)	P(2)-Pt(1)-P(3)	168.26(5)
Pt(1)–P(2)	2.2863(13)	P(1)-Pt(1)-P(2)	98.87(5)
Pt(1)–P(3)	2.2771(14)	P(1)-Pt(1)-P(3)	92.83(5)
P(1)-H(P1)	1.32(6)	Pt(1)-P(1)-C(1)	112.00(18)
P(1)–B(1)	1.953(7)	Pt(1)-P(1)-B(1)	119.8(2)
P(1)–C(1)	1.829(6)	C(1)-P(1)-H(P1)	98(3)
P(2)–C(7)	1.828(5)	B(1)-P(1)-C(1)	111.2(3)
P(2)–C(9)	1.824(6)	B(1)-P(1)-H(P1)	107(3)
P(2)–C(11)	1.836(5)	Pt(1)-P(1)-H(P1)	106(3)
P(3)–C(13)	1.831(6)		
P(3)–C(15)	1.820(6)		
P(3)–C(17)	1.831(7)		

the bonds Pt(1)–P(2) (2.2863(13) Å) and Pt(1)–P(3) (2.2771(14) Å) were found to be shorter than the Pt(1)–P(1) bond (2.3477(14) Å). Interestingly, the P(1)–B(1) bond length of 1.953(7) Å in **1** is longer than that in the parent adduct $PhPH_2 \cdot BH_3$ (1.924(4) Å).[14] The geometries around phosphorus and boron atoms in the phosphidoborane ligand are approximately tetrahedral, with angles around P(1) varying from 98(3)° to 119.8(2)°, and angles around B(1) varying from 100(5)° to 118(5)°. Complex **1** is the first structurally characterized example of a transition metal complex containing a primary phosphidoborane adduct.

For complex **2** (Figure 3), a structure analogous to that of **1** was found, with similar trends in bond lengths and angles (Table 2). Two of the ethyl substituents on P(2) (namely C(13), C(14) and C(15), C(16)) are disordered over two sites with the ratio of occupancies 0.54/0.46. Again, the hydride ligand could not be located during the X-ray analysis, but the wide P(2)-Pt(1)-P(3) angle of 160.22(12)° can be used to infer its presence. This angle is significantly smaller than that of **1** (168.26(5)°), presumably as a consequence of the greater steric bulk of a secondary phosphidoborane ligand over a primary ligand. In order to relieve the steric strain caused by the two phenyl groups, the two PEt_3 ligands are pushed away from the phosphidoborane ligand, thereby reducing the P(2)-Pt(1)-P(3) angle. The Pt–P bond lengths were found to follow the same trend as in **1**, with the Pt–PEt_3 bond lengths (2.253(3) Å and 2.256(2) Å) being significantly shorter than the Pt–($PPh_2 \cdot BH_3$) bond length (2.331(3) Å). The P–B bond length was found to be 1.925(11) Å.

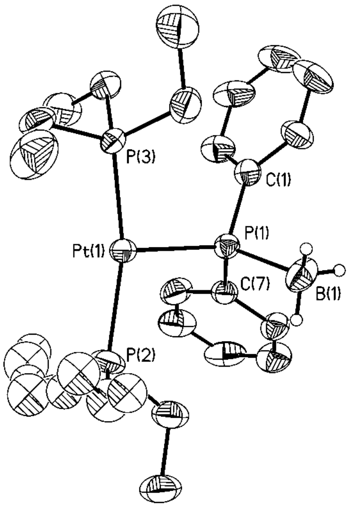

Figure 3. Molecular structure of *trans*-$[PtH(PPh_2 \cdot BH_3)(PEt_3)_2]$ (**2**). All hydrogen atoms bonded to carbon are omitted for clarity. Selected bond lengths and angles are presented in Table 2.

Table 2. Selected bond lengths [Å] and angles [°] for **2**.

Pt(1)–P(1)	2.331(3)	P(2)-Pt(1)-P(3)	160.22(12)
Pt(1)–P(2)	2.253(3)	P(1)-Pt(1)-P(2)	98.72(9)
Pt(1)–P(3)	2.256(2)	P(1)-Pt(1)-P(3)	99.10(9)
P(1)–B(1)	1.925(11)	Pt(1)-P(1)-C(1)	115.9(4)
P(1)–C(1)	1.757(9)	Pt(1)-P(1)-C(7)	109.7(3)
P(1)–C(7)	1.818(8)	Pt(1)-P(1)-B(1)	115.2(5)
		C(1)-P(1)-B(1)	106.8(6)
		C(7)-P(1)-B(1)	109.0(5)
		C(1)-P(1)-C(7)	98.9(4)

Transition metal complexes of secondary phosphine–borane adducts analogous to **2** are rare, with only two known cases to date. The first is a tetrahedral iron complex $[Fe(\eta^5\text{-}C_5Me_5)(CO)_2(PPh_2 \cdot BH_3)]$ synthesized from a nucleophilic metallation reaction between $Na[Fe(CO)_2(\eta^5\text{-}C_5Me_5)]$ and Ph_2PCl, followed by generation of the adduct through treatment with $BH_3 \cdot THF$.[28] The second is a square-planar palladium complex $[Pd(dppp)(C_6F_5)(PPh_2 \cdot BH_3)]$ (dppp = 1,3-bis(diphenylphosphino)propane) synthesized from an anionic phosphine–borane adduct $K[Ph_2P \cdot BH_3]$ and $[Pd(dppp)(C_6F_5)I]$.[29] This complex is also a proposed intermediate in the Pd-catalyzed coupling of secondary phosphine-boranes with aryl halides. In addition, transition-metal complexes containing a secondary phosphidoboratabenzene ligand have been synthesized and characterized by X-ray crystallography; namely, $[Fe(\eta^5\text{-}C_5H_5)(CO)_2(PPh_2 \cdot BC_5H_5)$, $[ZrH(\eta^5\text{-}C_5H_5)_2(PMe_3)(PPh_2 \cdot BC_5H_5)$, and $[Rh(PMe_3)_3(PPh_2 \cdot BC_5H_5)]$.[30] However, routes to these complexes all require a nucleophilic substitution step, rather than oxidative addition of the phosphine–borane adduct itself. Recently, the reaction of a transition-metal-complexed phosphine $[PH_3 \cdot W(CO)_5]$ with $[Pt(PPh_3)_2(C_2H_4)]$ has been found to yield $[PtH\{PH_2\text{-}W(CO)_5\}(PPh_3)_2]$, in which insertion of the Pt^0 center into the P–H bond of the phosphine has occurred.[31, 32] Only one other example of oxidative addition to transition metal centers is known for phosphine–borane adducts; however, it involves boron trihalide adducts rather than the hydridic borane (BH_3) adducts.[33] Reaction of *trans*-$[RhX(CO)(PEt_3)_2]$ (X = Br, I) with $PH_3 \cdot BY_3$ (Y = Cl, Br) yields the complexes $[RhHX(CO)(PEt_3)_2(PH_2 \cdot BY_3)]$, in which insertion of the transition metal into a P–H bond has occurred to yield an octahedral Rh complex. When X = NCS, reaction with $PH_3 \cdot BBr_3$ resulted in the formation of $[RhH(CO)(PH_2 \cdot BBr_3)_2(PEt_3)_2]$, in which a bis(phosphidotribromoborane) species is formed. However, because of the instability of these complexes at room temperature, no crystals suitable for X-ray analysis could be obtained,

Phosphine–borane ligand-exchange reaction between 2 and $PhPH_2 \cdot BH_3$: To further explore the reactivity of complexes **1** and **2**, the reaction with the adducts $Ph_2PH \cdot BH_3$ and $PhPH_2 \cdot BH_3$ was investigated in an attempt to induce P–B bond formation. The expected product from such a reaction would be a linear dimer of the type $BH_3\text{-}PPhR\text{-}BH_2\text{-}PPhRH$ (R = H or Ph). In the case of R = Ph, the linear dimer has been synthesized independently by Rh-catalyzed dehydrocoupling of $Ph_2PH \cdot BH_3$.[13, 14] Treatment of **1** with either one equivalent of $PhPH_2 \cdot BH_3$ or one equivalent of $Ph_2PH \cdot BH_3$ did not lead to a detectable reaction. Similarly, treatment of **2** with one equivalent of $Ph_2PH \cdot BH_3$ failed to lead to the intended coupling. However, the reaction of **2** with $PhPH_2 \cdot BH_3$ resulted in an exchange of the phosphidoborane ligands and the formation of **1** and $Ph_2PH \cdot BH_3$ [Eq. (5)]. The reaction

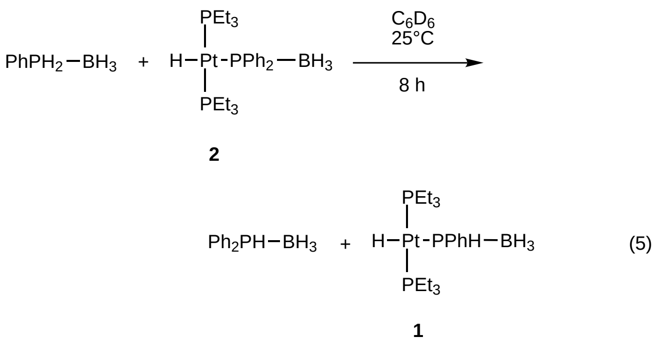

(5)

was followed by ^{31}P NMR; 100% conversion occurred after approximately 8 h. A similar reaction was attempted with **2** and *t*BuPH$_2$·BH$_3$; however, no exchange of the phosphine–borane ligands was observed in this case. A similar type of exchange reaction has been previously observed by Glueck and co-workers for terminal Pt^{II} phosphido complexes. They demonstrated that secondary phosphido complexes react with primary phosphines to yield primary phosphido complexes and secondary phosphines.[34] The driving force for the exchange was related to both the relative Pt–P bond strengths and also steric effects, because bonds to smaller phosphido ligands are more thermodynamically favored. In this case, complex **1** is thermodynamically favored because a primary phosphidoborane ligand is less sterically demanding than the corresponding secondary phosphidoborane ligand.[35] Evidence in support of this assertion is apparent in the crystal structures of **1** and **2**, in which the P-Pt-P angle is decreased by 8° owing to the sterically bulky secondary complex to result in more distortion of the ideal square-planar geometry.

Formation of *cis*-[PtH(PPh$_2$·BH$_3$)(depe)] (3) from *trans*-[PtH(PPh$_2$·BH$_3$)(PEt$_3$)$_2$] (2): Because the reactions of primary and secondary phosphine–borane adducts with the *trans* complexes **1** and **2** did not lead to the desired P–B bond formation by coupling chemistry, attempts were made to synthesize analogues of **1** and **2** with a *cis* geometry. It was hoped that P–B coupling by means of reductive elimination might occur more readily from a *cis* geometry than from a *trans* arrangement. Therefore, chelating phosphines were used in an attempt to create a structure in which the hydride ligand and the phosphidoborane ligand are arranged *cis* to one another. For example, 1:1 stoichiometric reactions of **2** and bis(diphenylphosphino)methane (dppm) resulted in no detectable reaction, whereas reaction with 1,2-bis(diphenylphosphino)ethane (dppe) yielded [Pt(dppe)$_2$] and the reductive elimination product Ph$_2$PH·BH$_3$, as well as unreacted **2**. When a 1:2 stoichiometry of **2**:dppe was used, full conversion to [Pt(dppe)$_2$] and Ph$_2$PH·BH$_3$ was observed by ^{31}P NMR. However, when a 1:1 mixture of **2** and 1,2-bis(diethylphosphino)ethane (depe) was allowed to react at room temperature, displacement of two PEt$_3$ ligands and binding of the depe ligand to the Pt center was detected by ^{31}P NMR spectroscopy. Subsequent workup of the reaction mixture yielded *cis*-[PtH(PPh$_2$·BH$_3$)(depe)] (**3**) as a white powder in 68% yield [Eq. (6)]. Characterization by multinuclear NMR spectroscopy was utilized to establish the structure of **3** and, in addition, an X-ray analysis confirmed the *cis* geometry. For example, the ^{31}P{^{1}H} NMR spectrum showed three sets of signals: 1) a doublet of doublets at $\delta = 63.7$, 2) a doublet of doublets at $\delta = 57.9$, and 3) a broad doublet of quartets at $\delta = -2.3$, all of which had associated ^{195}Pt satellites (Figure 4). This indicated the presence of three different phosphorus environments, which implies that the phosphorus nuclei of the depe ligand are nonequivalent and might be located in a *cis*/*trans* arrangement with respect to the phosphidoborane ligand. The resonance signal at $\delta = 63.7$ ppm was assigned to one PEt$_2$ group of the depe ligand which couples to two other phosphorus nuclei, one arranged *cis* (^2J(P,P$_{cis}$) = 4.5 Hz) and the other arranged *trans* (^2J(P,P$_{trans}$) = 276 Hz), and also showed ^{195}Pt satellites (^1J(P,Pt) = 2175 Hz). The resonance signal at $\delta = 57.9$ ppm was assigned to the other PEt$_2$ group of the depe ligand with coupling to two other phosphorus nuclei in a *cis* arrangement as indicated by the smaller coupling constants observed

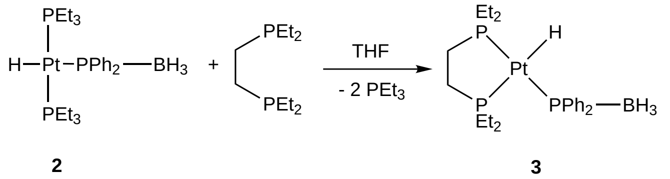

(6)

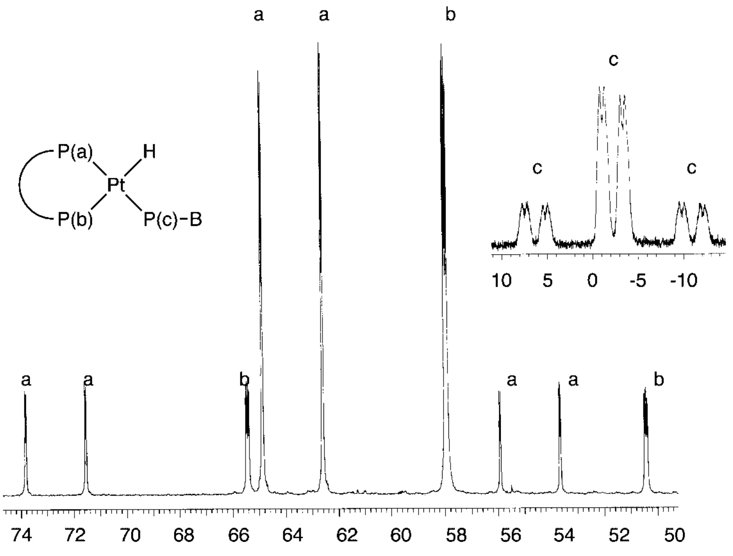

Figure 4. ^{31}P{^{1}H} NMR spectrum of *cis*-[PtH(PPh$_2$·BH$_3$)(depe)] (**3**). For P(a): ^2J(P,P$_{cis}$) = 4.5 Hz, ^2J(P,P$_{trans}$) = 276 Hz, ^1J(Pt,P) = 2175 Hz; P(b): ^2J(P,P$_{cis}$) = 4.5 Hz, ^2J(P,P$_{cis}$) = 5.1 Hz, ^1J(Pt,P) = 1823 Hz; P(c): ^2J(P,P$_{trans}$) = 276 Hz, ^1J(P,B) ≈ 63 Hz, ^1J(Pt,P) = 2094 Hz.

0947-6539/03/0901-0275 $ 20.00+.50/0

($^{2}J(\mathrm{P,P}_{cis}) = 4.5$ Hz and 5.1 Hz), as well as ^{195}Pt satellites ($^{1}J(\mathrm{P,Pt}) = 1823$ Hz). The broad doublet of quartets at $\delta = -2.3$ ppm is assigned to the phosphidoborane ligand, for which coupling to a *trans* phosphorus ($^{2}J(\mathrm{P,P}_{trans}) = 276$ Hz) gives rise to a doublet, while coupling to the boron yields a broad quartet ($^{1}J(\mathrm{P,B}) \approx 63$ Hz) in addition to ^{195}Pt satellites ($^{1}J(\mathrm{P,Pt}) = 2094$ Hz). Unfortunately, coupling to the other *cis* phosphorus (PEt_2) was not observed, presumably as a consequence of the broadness of the signal that is caused by coupling with the quadrupolar boron nucleus. The ^{11}B NMR spectrum showed a broad signal at $\delta = -32.1$ ppm, which is in the same region as the signals observed for **1** and **2**. Again, the key feature of the ^{1}H NMR spectrum was the low-frequency hydride resonance at $\delta = -1.74$ ppm that appeared as a doublet of doublets of doublets and arose from coupling to three different phosphorus nuclei. Smaller couplings were observed for the two *cis* phosphorus nuclei ($^{2}J(\mathrm{H,P}_{cis}) = 6.3$ Hz and 13.7 Hz), a larger coupling to the single *trans* phosphorus nucleus ($^{2}J(\mathrm{H,P}_{trans}) = 174$ Hz), and to ^{195}Pt ($^{1}J(\mathrm{H,Pt}) = 988$ Hz). All of this NMR evidence suggests the presence of one *trans* substituent (PEt_2) and two *cis* substituents (PEt_2 and $PPh_2 \cdot BH_3$) with respect to the hydride ligand.

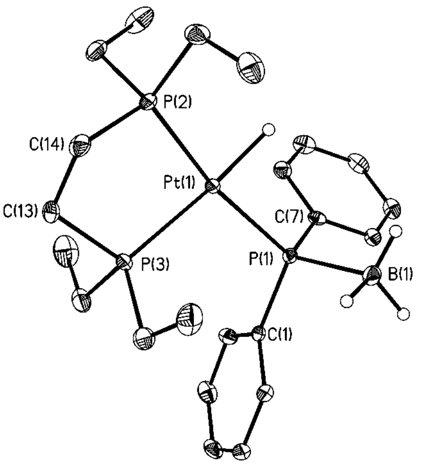

Figure 5. Molecular structure of *cis*-[PtH($PPh_2 \cdot BH_3$)(depe)] (**3**). All hydrogen atoms bonded to carbon are omitted for clarity. Selected bond lengths and angles are presented in Table 3.

Table 3. Selected bond lengths [Å] and angles [°] for **3**.

Pt(1)–P(1)	2.3170(11)	P(3)-Pt(1)-H(Pt1)	175.0(13)
Pt(1)–P(2)	2.2589(11)	P(2)-Pt(1)-P(3)	86.00(4)
Pt(1)–P(3)	2.2969(11)	P(1)-Pt(1)-P(2)	170.07(4)
Pt(1)–H(Pt(1))	1.59(4)	P(1)-Pt(1)-P(3)	102.58(4)
P(1)–C(1)	1.830(4)	Pt(1)-P(1)-C(7)	111.15(15)
P(1)–C(7)	1.835(4)	Pt(1)-P(1)-B(1)	111.27(17)
P(1)–B(1)	1.956(5)	Pt(1)-P(1)-C(1)	116.91(14)
C(13)–C(14)	1.524(6)		

X-ray crystallographic analysis of 3: To confirm the structure of **3**, a single-crystal X-ray analysis was performed. The molecular structure of **3** is shown in Figure 5, bond lengths and angles are given in Table 3. In contrast to structures **1** and **2**, the hydride ligand was located during the course of this study, and was included in the refinement. In a similar manner to **1** and **2**, the geometry around Pt in **3** is distorted square-planar, with large angles between the *trans* substituents of 175.0(13)° (P(3)-Pt(1)-H(Pt(1))) and 170.07(4)° (P(1)-Pt(1)-P(2)). The angles between the *cis* substituents are all close to 90°, with the bite angle of the depe ligand being 86.00(4)°. The Pt(1)–H(Pt(1)) bond length was found to be 1.59(4) Å. This is much longer than the bond length of 1.29(16) Å found in the structure of *cis*-[PtH{P(O)Ph_2}{PPh_2(OH)}(PEt_3)], which has a similar arrangement of three phosphorus and one hydrogen atom located around the metal center.[21] The Pt–P bond length of the phosphidoborane ligand was determined to be 2.3170(11) Å, which is slightly shorter than the bond length of 2.331(3) Å found in the structure of **2**. The Pt(1)–P(2) and Pt(1)–P(3) bond lengths of the chelating phosphine were found to be 2.2589(11) Å and 2.2969(11) Å, respectively. The longer Pt(1)–P(3) bond length may arise as a consequence of the hydride ligand having a greater *trans* influence than the phosphidoborane ligand. A similar trend in Pt–P bond lengths was observed in the crystal structure of *cis*-[PtH{P(O)Ph_2}{PPh_2(OH)}(PEt_3)].[21] The P(1)–B(1) bond length of 1.956(5) Å is longer than that in structure **2** (1.925(11) Å), which also has a secondary phosphidoborane ligand bearing two phenyl substituents.

Phosphine–borane ligand-exchange reaction between 3 and $PhPH_2 \cdot BH_3$: The reactivity of **3** with primary and secondary phosphine–borane adducts was explored with the hope of forming a new P–B bond by means of reductive elimination. When **3** was treated with one equivalent of $Ph_2PH \cdot BH_3$, no reaction was detected in solution by ^{31}P NMR. However, when **3** was treated with one equivalent of $PhPH_2 \cdot BH_3$, an exchange of the phosphine-borane ligands was observed after 3 h with the formation of the complex *cis*-[PtH($PPhH \cdot BH_3$)(depe)] (**4**) and $Ph_2PH \cdot BH_3$ [Eq. (7)]. The ^{31}P NMR spectrum showed the formation of three new resonances

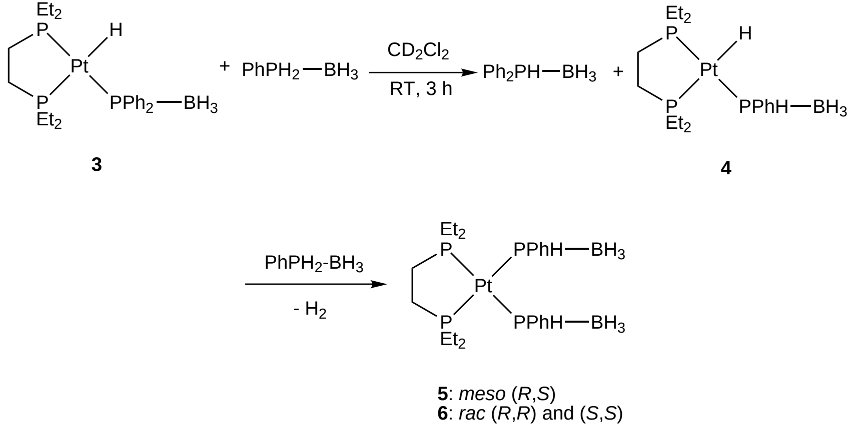

(7)

assigned to **4**: 1) a broad doublet at $\delta = -51.1$ ppm (^2J(P,P) = 272 Hz) with ^{195}Pt satellites (^1J(P,Pt) = 1856 Hz) assigned to the PhPH · BH$_3$ moiety, 2) a doublet of doublets at δ = 56.7 ppm (^2J(P,P) = 5.1 Hz and 15.5 Hz) with ^{195}Pt satellites (^1J(P,Pt) = 1762 Hz) assigned to the depe PEt$_2$ group that is *cis* to the PPhH · BH$_3$ moiety, and 3) a doublet of doublets at δ = 62.4 ppm (^2J(P,P) = 5.1 Hz and 272 Hz) with ^{195}Pt satellites (^1J(P,Pt) = 2238 Hz) assigned to the other depe PEt$_2$ group that is arranged *trans* to the PPhH · BH$_3$ moiety. The ^{11}B NMR spectrum of the reaction mixture showed a new resonance at $\delta = -34.4$ ppm, which is similar to those seen for complexes **1**–**3**. The ^{1}H NMR spectrum showed two distinct resonance signals associated with **4**: 1) a broad doublet at δ = 5.06 (^1J(H,P) = 310 Hz) assigned to the PH proton, and 2) a doublet of multiplets at $\delta = -1.88$ ppm (^2J(H,P) = 171 Hz) with ^{195}Pt satellites (^1J(H,Pt) = 980 Hz) assigned to the hydride ligand. The coupling pattern of the latter signal would be expected to be similar to that seen in **3**, which occurs as a doublet of doublet of doublets, arising from a coupling to two *cis* and one *trans* phosphorus nuclei. However, the two *cis* couplings are not well-resolved in **4** and result in a doublet of multiplets instead.

Complex **4** was observed to undergo further reaction with PhPH$_2$ · BH$_3$ in solution and two new products, **5** and **6**, were detected after 8 h. After 28 h of reaction time, the solution contained a mixture of complexes **4** (40 %), **5** (30 %), **6** (30 %), and Ph$_2$PH · BH$_3$ with no further conversion at longer reaction times. However, reaction of two equivalents of PhPH$_2$ · BH$_3$ with **3** resulted in the quantitative formation of **5** and **6** in a 1:1 ratio after 22 h. An isolated sample of **5** was obtained by recrystallization and was fully characterized by NMR spectroscopy and also single-crystal X-ray diffraction (see below). The resulting data identified **5** as the (*R*,*S*) isomer of *cis*-[Pt(PPhH · BH$_3$)$_2$(depe)]. As each phosphorus present in the phosphidoborane ligands has four unique substituents (Pt, Ph, B, and H), there are two chiral centers and either *meso* or *rac* forms are expected. The ^{31}P NMR spectrum of **5** showed two resonance signals associated with the *meso* form: 1) a broad doublet at $\delta = -40.3$ ppm (^2J(P,P) = 241 Hz) with ^{195}Pt satellites (^1J(P,Pt) = 1717 Hz) assigned to the PhPH · BH$_3$ moiety, and 2) a multiplet at δ = 58.5 ppm with ^{195}Pt satellites (^1J(P,Pt) = 2099 Hz) assigned to the depe ligand. The observed pattern of the multiplet (Figure 6 a) occurs as a result of a non-first order AA′XX′ spin system that is due to the chiral phosphorus centers of the phosphidoborane moieties. A computer simulation (Figure 6 b) was obtained by fixing the *trans* coupling constant at ^2J(A,X′) = ^2J(A′,X) = 230 Hz (as measured from the spectrum) and varying the *cis* coupling constants, which refined at ^2J(A,X) = ^2J(A′,X′) = −20 Hz, ^2J(X,X′) = 8 Hz and ^2J(A,A′) = 0 Hz. It has been observed that, for spin-simulated ^{31}P NMR spectra of complexes containing four co-planar phosphorus nuclei, the *cis* and *trans* ^2J(P,P) coupling constants are required to have opposite signs.[36c] The complex *cis*-[Pt(μ-PPhH)$_2$(Mo(CO)$_4$)(dppe)][36] also has an AA′XX′ spin system that contains two chiral phosphido groups and which possesses a similar ^{31}P NMR coupling pattern as those observed for **5** and **6**. The ^{11}B NMR spectrum shows a broad signal at $\delta = -37.6$ ppm, while the ^{1}H NMR spectrum shows a broad doublet at δ = 4.53 ppm (^1J(H,P) = 328 Hz) assigned to the PH proton.

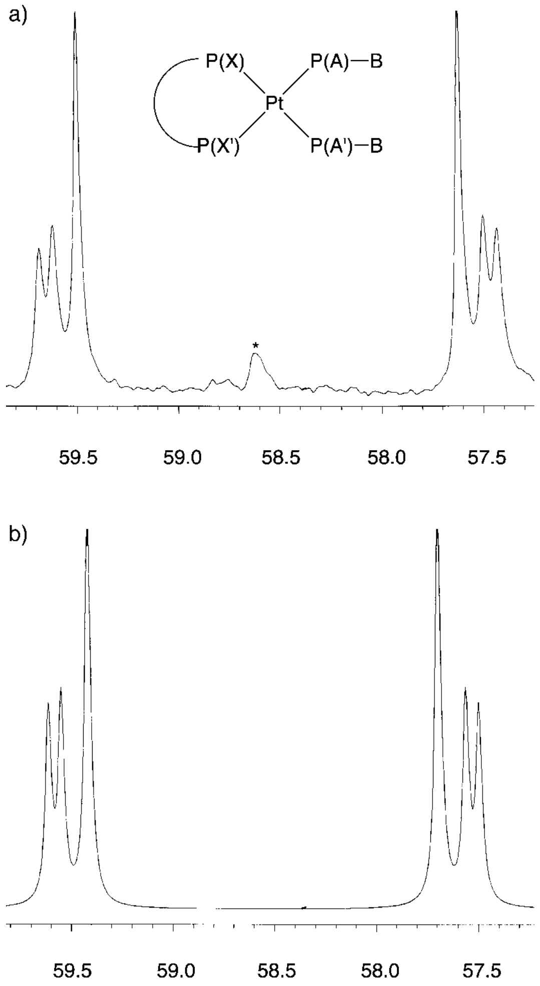

Figure 6. a) Selected region (depe) of the ^{31}P{^{1}H} NMR spectrum of (*R*,*S*)-*cis*-[Pt(PPhH · BH$_3$)$_2$(depe)] (**5**) along with b) computer simulation of the AA′XX′ spin system with ^2J(A,X′) = ^2J(A′,X) = 230 Hz, ^2J(A,X) = ^2J(A′,X′) = −20 Hz, ^2J(X,X′) = 8 Hz and ^2J(A,A′) = 0 Hz. The associated ^{195}Pt satellites are omitted for clarity. Unidentified impurities in the spectrum are denoted by *.

Identification of **5** as the *meso* form of *cis*-[Pt(PPhH · BH$_3$)$_2$(depe)] allowed **6** to be assigned as a racemic mixture of the (*R*,*R*) and (*S*,*S*) enantiomers. The only spectroscopic difference between *rac*-**6** and *meso*-**5** is observed in the ^{31}P{^{1}H} NMR spectrum: the broad doublet assigned to the phosphidoborane moieties was found to be shifted to $\delta = -27.5$ ppm ($\delta = -40.3$ for **5**) while the multiplet assigned to the depe ligand occurred at δ = 57.6 ppm (δ = 58.5 for **5**).

Complexes **5** and **6** can also be formed from the reaction of [(depe)PtCl$_2$] and Li[PPhH · BH$_3$] in CH$_2$Cl$_2$. This route requires less steps than the aforementioned sequence of reactions and the only byproduct is LiCl, which is easily removed by filtration. A second possible route to **4** from the reaction of the primary complex **1** with depe was also investigated; however, the only identified products from the reaction were equal mixtures of complexes **5** and **6**. The presence of **4** in solution could not be detected by ^{31}P NMR, even as a minor byproduct.

X-ray crystallographic analysis of 5: The molecular structure of **5** is shown in Figure 7, bond lengths and angles are given in Table 4. Disorder in the ethane bridge of the depe ligand was observed, with the occupancies of C(1)/C(1*) and C(2)/C(2*) found to be 0.50/0.50. The hydrogen atoms attached to the boron and phosphorus atoms of the phosphidoborane moieties were not located and were therefore included in calculated positions. As in the structures of **1**–**3**, the geometry around Pt is distorted square-planar with large angles of 175.43(12)° and 174.06(13)° between the *trans* substituents. The bite angle of the depe ligand (86.04(13)°) was found to be nearly identical to the value found for **3** (86.00(4)°). The Pt–P bond lengths of the phosphidoborane moiety were found to be consistent with those found for **1**, and have values of 2.335(3) Å for Pt(1)–P(3) and 2.354(3) Å for Pt(1)–P(4). In the absence of a large *trans* effect from a hydride ligand, the Pt–P bonds of the depe ligand were found to have equal lengths of 2.293(3) Å. The P–B bond lengths of the phosphidoborane moieties were found to have values of 1.933(17) Å for P(3)–B(1) and 1.958(17) Å for P(4)–B(2), and are consistent with the P–B bond lengths found in **1** (1.953(7) Å). The absolute configurations at the chiral phosphorus atoms were determined to be (*R*) for P(3) and (*S*) for P(4). Complex **5** represents the first structurally characterized example of a transition metal complex containing two primary phosphidoborane ligands.

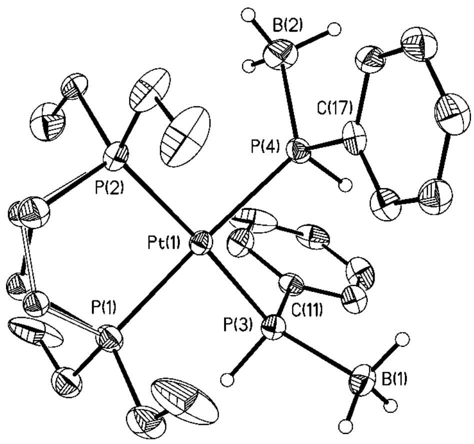

Figure 7. Molecular structure of (*R*,*S*)-*cis*-[Pt(PPhH · BH_3)$_2$(depe)] (**5**). All hydrogen atoms bonded to carbon are omitted for clarity. Selected bond lengths and angles are presented in Table 4.)

Table 4. Selected bond lengths [Å] and angles [°] for **5**.

Pt(1)–P(1)	2.293(3)	P(1)-Pt(1)-P(2)	86.04(13)
Pt(1)–P(2)	2.293(3)	P(1)-Pt(1)-P(3)	91.27(12)
Pt(1)–P(3)	2.335(3)	P(1)-Pt(1)-P(4)	174.06(13)
Pt(1)–P(4)	2.354(3)	P(2)-Pt(1)-P(3)	175.43(12)
P(3)–B(1)	1.933(17)	P(2)-Pt(1)-P(4)	94.00(12)
P(4)–B(2)	1.958(17)	P(3)-Pt(1)-P(4)	89.05(12)
P(3)–C(11)	1.832(14)		
P(4)–C(17)	1.819(14)		

Mechanism of the formation of 5 and 6: The formation of **5** and **6** from the intermediate complex **4** may result from a dehydrocoupling reaction between the platinum hydride and a second equivalent of $PhPH_2 \cdot BH_3$. The reaction may initially involve oxidative addition of the P–H bond of the adduct to give a Pt^{IV} species, followed by reductive elimination of dihydrogen to generate the disubstituted complexes **5** and **6**. However, evidence for a Pt^{IV} intermediate was not detected when the reaction was monitored by NMR spectroscopy. This suggests that the process is very fast, although a σ-bond metathesis mechanism involving a four-centered transition state should also be considered. To the best of our knowledge, there are no other reactions of this type which involve mononuclear platinum hydride complexes and either primary or secondary phosphines or phosphine–borane adducts. An analogous reaction in which a dinuclear platinum hydride complex reacts to form H_2 was demonstrated by Puddephatt et al. The complex [Pt_2(*μ*-H)Me_6(bu_2bpy)$_2$]OTf (bu_2bpy = 4,4′-di-*tert*-butyl-2,2′-bipyridine, OTf = SO_3CF_3) was shown to react with acids, such as HCl, CF_3COOH, and HSPh, to formally generate H_2 (not observed) and the substituted complexes.[37, 38]

Conclusion

Oxidative addition of the P–H bonds of primary and secondary phosphine–borane adducts at Pt^0 centers has been found to yield the *trans* complexes **1** and **2**. Subsequent P–B bond coupling could not be induced by further treatment with $PhPRH \cdot BH_3$; however, an unusual phosphidoborane ligand-exchange reaction between **2** and $PhPH_2 \cdot BH_3$ to yield **1** and $Ph_2PH \cdot BH_3$ was observed. This exchange process was dependent upon steric factors. The primary phosphidoborane Pt^{II} complex **1** is thermodynamically favored over the more sterically hindered secondary complex **2**. Addition of a chelating phosphine (depe) to **2** resulted in the displacement of the PEt_3 ligands to yield complex **3**, in which the hydrido and phosphidoborane ligands are arranged *cis* to one another. The only route to the analogous complex **4** found in this work involves the phosphidoborane ligand-exchange reaction between **3** and $PhPH_2 \cdot BH_3$. Complex **4** undergoes further reaction with $PhPH_2 \cdot BH_3$ to give **5** and **6**, which are the *meso* and *rac* forms of the corresponding disubstituted phosphidoborane complex. Complex **5** represents the first structurally characterized example of a transition metal complex containing two primary phosphidoborane ligands. The reaction of **4** with $PhPH_2 \cdot BH_3$ can be formally considered a novel dehydrocoupling reaction with the formation of H_2 and a new Pt–P bond.

The lack of any detectable P–B bond-formation chemistry during the reaction of **1**–**4** with phosphine–borane adducts suggests that other mechanisms for the catalytic dehydrocoupling chemistry, which do not involve the initial formation of M–P bonds, may need to be considered. We are now also exploring the reactivity of phosphine–borane adducts with other late transition metal centers and are addressing the possibility that metal-boryl[23] species may be productively involved in the catalytic cycle.

Experimental Section

General procedures and materials: All reactions and product manipulations were performed under an atmosphere of dry nitrogen by means of standard Schlenk techniques or in a glovebox under an inert atmosphere. All solvents were dried over appropriate drying agents, such as Na/benzophenone (toluene, hexanes, THF) or CaH_2 (CH_2Cl_2), and distilled prior to use. $BH_3 \cdot SMe_2$, $BH_3 \cdot THF$ (1 M in THF), dppe, dppm, BuLi (1.6 M in hexanes) (Aldrich), $PhPH_2$, Ph_2PH, Et_3P, depe (Strem Chemicals), as well as $PtCl_2$ and K_2PtCl_4 (Pressure Chemical Co.) were purchased and used as received. $Ph_2PH \cdot BH_3$ was prepared by means of a procedure analogous to that used for $PhPH_2 \cdot BH_3$.[39] [Pt(depe)Cl_2][40] and [Pt(PEt_3)$_4$][41] were prepared according to literature procedures. [Pt(PEt_3)$_3$] was obtained by heating [Pt(PEt_3)$_4$] at 60 °C in vacuo for 16 h.

Equipment: NMR spectra were recorded on either a Varian Gemini 300 MHz or a Varian Unity 400 MHz (^{13}C) spectrometer. Chemical shifts are reported relative to residual protonated solvent resonances (^1H, ^{13}C) or external standards: $BF_3 \cdot Et_2O$ (^{11}B), H_3PO_4 (^{31}P), or K_2PtCl_6 (^{195}Pt). All spectra were obtained at room temperature (25 °C) unless otherwise specified. Mass spectra were obtained with a VG 70–250S mass spectrometer operating in the electron impact (EI) mode. Melting point determinations were performed in sealed capillaries and are uncorrected. Infrared spectra were recorded on a Nicolet Magna 550 FT-IR instrument as Nujol mulls between KBr plates. Elemental analyses were performed by Quantitative Technologies Inc., Whitehouse, NJ (USA).

X-ray structural characterization: Crystallographic data and the summary of data collection and refinement for structures **1**, **2**, **3**, and **5** are presented in Table 5. Diffraction data were collected on a Nonius Kappa-CCD with graphite-monochromated $Mo_{K\alpha}$ radiation ($\lambda = 0.71073$ Å). The data were integrated and scaled with the Denzo-SMN package.[42] The structures were solved and refined with the SHELXTL-PC V5.1 software package.[43] Refinement was by full-matrix least-squares on F^2 of all data (negative intensities included). All molecular structures are presented with thermal ellipsoids at a 30 % probability level. In all structures, hydrogens bonded to carbon atoms were included in calculated positions and treated as riding atoms. For structures **1** and **3**, the hydrogen atoms attached to boron and phosphorus or platinum (**3**) were located and refined with isotropic thermal parameters. For structures **2** and **5**, the hydrogen atoms attached to boron and phosphorus were located and were included in calculated positions and treated as riding atoms.

CCDC-1821620 (**1**), CCDC-189321 (**2**), CCDC-189322 (**3**), and CCDC-189323 (**5**) contain the supplementary crystallographic data for this paper. These data can be obtained free of charge via www.ccdc.cam.ac.uk/conts/retrieving.html (or from the Cambridge Crystallographic Data Centre, 12 Union Road, Cambridge CB2 1EZ, UK; fax: (+44) 1223-336033; or deposit@ccdc.cam.ac.uk).

Synthesis of *trans*-[PtH(PPhH·BH_3)(PEt_3)$_2$] (1): [Pt(PEt_3)$_3$] (453 mg, 0.82 mmol) in toluene (15 mL) was added dropwise to a solution of $PhPH_2 \cdot BH_3$ (134 mg, 1.08 mmol) in toluene (10 mL), and the mixture was heated to 60 °C for 21 h. The solvent was removed under vacuum, and the oily orange residue extracted with hot hexanes (30 mL) and filtered. The solvent was removed under vacuum to give a yellow powder. X-ray quality crystals of **1** were obtained overnight from a hexanes solution at −20 °C. Yield 106 mg (23 %); m.p. 67–68 °C; ^1H NMR (300 MHz, $CDCl_3$): $\delta = 7.76–7.70$ (m; Ph), 7.26–7.19 (m; Ph), 4.39 (d, $^1J(H,P) = 299$ Hz; PH), 1.80 (m; CH_2), 1.03 (m; CH_3), −5.74 ppm (dt, $^2J(H,P_{trans}) = 125$ Hz, $^2J(H,P_{cis}) = 15$ Hz, $^1J(H,Pt) = 872$ Hz; PtH); $^{11}B\{^1H\}$ NMR (96 MHz, $CDCl_3$): $\delta = -33.2$ ppm (br); $^{13}C\{^1H\}$ NMR (75 MHz, $CDCl_3$): $\delta = 137.6$ (d, $^1J(C,P) = 30$ Hz; *ipso*-Ar), 134.6 (d, $J(C,P) = 8$ Hz; Ar), 128.1 (Ar), 127.6 (d, $J(C,P) = 8$ Hz; Ar), 19.2 (m; CH_2), 8.9 ppm (m; CH_3); ^{31}P NMR (121 MHz, $CDCl_3$): $\delta = 17.9$ (d, $^2J(P,P) = 19$ Hz, $^1J(P,Pt) = 2572$ Hz; PEt_3), −48.7 ppm (br dq, $^1J(P,H) = 299$ Hz, $^1J(P,B) \approx 55$ Hz, $^1J(P,Pt) = 1440$ Hz; PHPh); ^{195}Pt NMR (64 MHz, $CDCl_3$): $\delta = -3541$ ppm (tdd, $^1J(Pt,P) = 2573$ Hz, $^1J(Pt,P) = 1462$ Hz, $^1J(Pt,H) = 820$ Hz); IR (Nujol): $\tilde{\nu} = 2350$ (BH), 2022 (PtH) cm^{-1}; EI-MS (70 eV): *m*/*z* (%): 541 (1) $[M - BH_3]^+$, 118 (100) [PEt_3]; elemental analysis calcd (%) for $C_{18}H_{40}BP_3Pt$: C 38.93, H 7.26; found: C 38.95, H 7.17.

Synthesis of *trans*-[PtH($PPh_2 \cdot BH_3$)(PEt_3)$_2$] (2): [Pt(PEt_3)$_3$] (243 mg, 0.44 mmol) in toluene (10 mL) was added dropwise to a solution of $Ph_2PH \cdot BH_3$ (88 mg, 0.44 mmol) in toluene (15 mL), and the mixture was heated to 60 °C for 8 h. The solvent was removed under vacuum, and the oily orange residue was extracted with hot hexanes (15 mL) and filtered.

Table 5. Crystallographic data and summary of data collection and refinement for structures **1**–**3** and **5**.

	1	**2**	**3**	**5**
empirical formula	$C_{18}H_{40}BP_3Pt$	$C_{24}H_{44}BP_3Pt$	$C_{22}H_{38}BP_3Pt$	$C_{22}H_{42}B_2P_4Pt$
fw	555.31	631.40	601.33	647.15
T [K]	150(1)	293(2)	150(1)	150(1)
λ [Å]	0.71073	0.71073	0.71073	0.71073
crystal system	monoclinic	orthorhombic	monoclinic	orthorhombic
space group	$C2/c$	$Pna2_1$	$P2_1/c$	$P2_12_12_1$
crystal size [mm]	0.15 × 0.15 × 0.10	0.25 × 0.23 × 0.20	0.25 × 0.23 × 0.20	0.30 × 0.13 × 0.05
a [Å]	27.1904(13)	18.8758(5)	10.2932(3)	9.2179(5)
b [Å]	9.8355(7)	9.1055(2)	15.3514(4)	17.3840(9)
c [Å]	19.0955(11)	15.9449(4)	16.5890(4)	17.5273(9)
α [°]	90	90	90	90
β [°]	110.777(3)	90	99.749(1)	90
γ [°]	90	90	90	90
V [Å^3]	4774.6(5)	2740.51(12)	2583.46(12)	2808.6(3)
Z	8	4	4	4
D_C [g cm^{-3}]	1.545	1.530	1.546	1.530
μ [mm^{-1}]	6.077	5.304	5.622	5.231
$F(000)$	2206	1264	1192	1288
Θ range [°]	2.62–27.51	4.14–26.68	2.55–25.02	3.42–25.01
index ranges	$0 \leq h \leq 35$	$-24 \leq h \leq 23$	$0 \leq h \leq 12$	$-9 \leq h \leq 10$
	$0 \leq k \leq 12$	$-11 \leq k \leq 11$	$0 \leq k \leq 18$	$-20 \leq k \leq 20$
	$-24 \leq l \leq 23$	$-20 \leq l \leq 20$	$-19 \leq l \leq 19$	$-20 \leq l \leq 20$
reflections collected	51791	22765	15075	11095
indexed reflections	5176	5521	4551	4868
R_{int}	0.063	0.065	0.047	0.0725
GoF on F^2	1.042	1.063	1.060	1.125
R_1[a] $[(I > 2\sigma(I)]$	0.0387	0.0393	0.0268	0.0554
$wR2$[b] (all data)	0.0969	0.1055	0.0603	0.1445
peak/hole [e Å^3]	1.728/−2.476	1.681/−1.999	1.335/−0.937	2.602/−1.788

[a] $R1 = \Sigma||F_0| - |F_C||/\Sigma|F_0|$. [b] $wR2 = \{\Sigma[w(F_0^2 - F_C^2)^2]/\Sigma[w(F_0^2)^2]\}^{1/2}$

X-ray quality orange crystals of **2** formed overnight at room temperature. Yield 175 mg (63 %); m.p. 113.5 – 114 °C; ^{1}H NMR (300 MHz, C_6D_6): $\delta =$ 8.26 – 8.14 (m; Ph), 7.26 – 7.00 (m; Ph), 3.0 – 1.9 (br q; BH_3), 1.48 (m; CH_2), 0.93 (m; CH_3), – 6.75 ppm (dt, $^2J(H,P_{trans}) = 124$ Hz, $^2J(H,P_{cis}) = 17$ Hz, $^1J(H,Pt) = 805$ Hz, PtH); $^{11}B\{^1H\}$ NMR (96 MHz, C_6D_6): $\delta = -31.4$ ppm (br); $^{13}C\{^1H\}$ NMR (75 MHz, C_6D_6): $\delta = 144.8$ (d, $^1J(C,P) = 27$ Hz; *ipso*-Ar), 135.1 (m; Ar), 19.9 (m; CH_2), 9.3 ppm (m; CH_3); $^{31}P\{^1H\}$ NMR (121 MHz, C_6D_6): $\delta = 16.7$ (d, $^2J(P,P) = 17$ Hz, $^1J(P,Pt) = 2648$ Hz; PEt_3), – 3.7 ppm (br, $^1J(P,Pt) = 1575$ Hz; PPh_2); ^{195}Pt NMR (64 MHz, C_6D_6): $\delta = -3450$ ppm (tdd, $^1J(Pt,P) = 2660$ Hz, $^1J(Pt,P) = 1643$ Hz, $^1J(Pt,H) = 789$ Hz); IR (Nujol): $\tilde{\nu} = 2341$ (BH), 2009 (PtH) cm^{-1}; EI-MS (70 eV): *m*/*z* (%): 617 (21) $[M - BH_3]^+$, 62 (100) $[H_2PEt]$; elemental analysis calcd (%) for $C_{24}H_{44}BP_3Pt$: C 45.65, H 7.02; found: C 45.86, H 6.98.

Exchange reaction between 2 and $PhPH_2 \cdot BH_3$: A solution of $PhPH_2 \cdot BH_3$ (6 mg, 0.04 mmol) in C_6D_6 was added to a solution of **2** (29 mg, 0.04 mmol) in C_6D_6 in a 5-mm NMR tube. The reaction was monitored periodically by $^{31}P\{^1H\}$ NMR spectroscopy. Full conversion to **1** and $Ph_2PH \cdot BH_3$ was achieved after 8 h at room temperature.

Reaction of 2 and dppm: dppm (35 mg, 0.09 mmol) was added to a solution of **2** (58 mg, 0.09 mmol) in C_6D_6 in a 5-mm NMR tube. After 2 h at room temperature, the $^{31}P\{^1H\}$ NMR spectrum indicated that no reaction had occurred. A second equivalent of dppm was added (34 mg, 0.09 mmol) and the $^{31}P\{^1H\}$ NMR spectrum again showed no reaction.

Reaction of 2 and dppe: dppe (22 mg, 0.06 mmol) in C_6D_6 was added to a solution of **2** (35 mg, 0.05 mmol) in C_6D_6 in a 5-mm NMR tube. After 15 min at room temperature, the $^{31}P\{^1H\}$ NMR spectrum showed the presence of $[Pt(dppe)_2]$ ($\delta = 31.6$ ppm, $^1J(Pt,P) = 3729$ Hz; literature value $\delta = 30.2$ ppm, $^1J(Pt,P) = 3728$ Hz),[44] PEt_3 ($\delta = -18.6$ ppm) and $Ph_2PH \cdot BH_3$ ($\delta = 2.9$) as well as unreacted **2**. Another equivalent of dppe was added (23 mg, 0.05 mmol) and the $^{31}P\{^1H\}$ NMR spectrum showed full conversion to $[Pt(dppe)_2]$, PEt_3, and $Ph_2PH \cdot BH_3$.

Synthesis of *cis*-$[PtH(PPh_2 \cdot BH_3)(depe)]$ (3): depe (33 mg, 0.16 mmol) in THF (2 mL) was added to a solution of **2** (97 mg, 0.15 mmol) in THF (5 mL) at room temperature, and the mixture was stirred for 1 h. All volatiles were removed under vacuum, and the resulting solid was dissolved in toluene (5 mL) to give a yellow solution and a white powder **3**. The solution was carefully decanted and the powder was washed with toluene (2 × 5 mL) and dried in vacuo overnight. X-ray quality crystals of **3** were obtained from slow evaporation of a THF solution at room temperature. Yield 63 mg (68 %); m.p. 179 – 181 °C; ^{1}H NMR (300 MHz, $[D_8]$THF): $\delta =$ 7.80 – 7.34 (m; Ph), 7.16 – 7.08 (m; Ph), 2.0 – 0.8 (br; BH_3), 1.99 – 1.67 (m; depe and Et CH_2), 1.20 – 0.83 (m; CH_3), – 1.74 (ddd, $^2J(H,P_{trans}) = 174$ Hz, $^2J(H,P_{cis}) = 14$ Hz, $^2J(H,P_{cis}) = 6.3$ Hz, $^1J(H,Pt) = 988$ Hz; PtH); $^{11}B\{^1H\}$ NMR (96 MHz, $[D_8]$THF): $\delta = -32.1$ ppm (br); $^{13}C\{^1H\}$ NMR (75 MHz, $[D_8]$THF): $\delta = 145.0$ (d, $^1J(C,P) = 32$ Hz; *ipso*-Ar), 135.3 (m; Ar), 128.0 (Ar), 127.7 (Ar), 27.1 – 26.5 (m; depe CH_2), 21.9 – 19.6 (m; CH_2), 10.3 – 9.3 ppm (m; CH_3); $^{31}P\{^1H\}$ NMR (121 MHz, $[D_8]$THF): $\delta = 63.7$ (dd, $^2J(P,P_{cis}) = 4.5$ Hz, $^2J(P,P_{trans}) = 276$ Hz, $^1J(P,Pt) = 2175$ Hz; PEt_2), 57.9 (dd, $^2J(P,P_{cis}) = 4.5$ Hz, $^2J(P,P_{cis}) = 5.1$ Hz, $^1J(P,Pt) = 1823$ Hz; PEt_2), – 2.3 ppm (br dq, $^2J(P,P_{trans}) = 276$ Hz, $^1J(P,B) \approx 63$ Hz, $^1J(P,Pt = 2094$ Hz; PPh_2); EI-MS (70 eV): *m*/*z* (%): 587 (100) $[M - BH_3]^+$; elemental analysis calcd (%) for $C_{22}H_{38}BP_3Pt$: C 43.94, H 6.37; found: C 43.87, H 6.25.

Exchange reaction between 3 and one equivalent of $PhPH_2 \cdot BH_3$; synthesis of *cis*-$[PtH(PPhH \cdot BH_3)(depe)]$ (4): A solution of $PhPH_2 \cdot BH_3$ (15 mg, 0.12 mmol) in CD_2Cl_2 was added to a solution of **3** (63 mg, 0.11 mmol) in CD_2Cl_2 in a 5-mm NMR tube. The reaction was monitored periodically by ^{31}P, ^{11}B, and ^{1}H NMR. After 3 h at room temperature, the presence of **4** and $Ph_2PH \cdot BH_3$ was detected in the solution.

$Ph_2PH \cdot BH_3$: ^{1}H NMR (300 MHz, CD_2Cl_2): $\delta = 6.33$ ppm (dq, $^1J(P,H) = 381$ Hz, $^3J(H,H) = 6.9$ Hz; PH); $^{11}B\{^1H\}$ NMR (96 MHz, CD_2Cl_2): $\delta = -40.4$ ppm (d, $^1J(B,P) = 44$ Hz); $^{31}P\{^1H\}$ NMR (121 MHz, CD_2Cl_2): $\delta = 1.87$ ppm (q, br).

cis-$[PtH(PPhH \cdot BH_3)(depe)]$ ***4***: Selected ^{1}H NMR (300 MHz, CD_2Cl_2): $\delta = 5.06$ (br d, $^1J(P,H) = 310$ Hz; PH), – 1.88 ppm (dm, $^2J(H,P_{trans}) = 171$ Hz, $^1J(H,Pt) = 980$ Hz; PtH); $^{11}B\{^1H\}$ NMR (96 MHz, CD_2Cl_2): $\delta = -34.4$ ppm (d, $^1J(B,P) = 47$ Hz); $^{31}P\{^1H\}$ NMR (121 MHz, CD_2Cl_2): $\delta = 62.4$ (dd, $^2J(P,P_{cis}) = 5.1$ Hz, $^2J(P,P_{trans}) = 272$ Hz, $^1J(P,Pt) = 2238$ Hz; PEt_2), 56.7 (dd, $^2J(P,P_{cis}) = 5.1$ Hz, $^2J(P,P_{cis}) = 15.5$ Hz, $^1J(P,Pt) = 1762$ Hz; PEt_2), – 51.1 ppm (d, $^2J(P,P_{trans}) = 272$ Hz, $^1J(P,Pt) = 1856$ Hz; PhPH). After 8 h, the formation of two new products **5** and **6** was observed in the NMR spectra, in addition to signals associated with complex **4** and unreacted **3**. The reaction was left to proceed for a further 20 h at room temperature after which time the NMR spectra indicated full conversion of **3** to a mixture of **4** (40 %), **5** (30 %), and **6** (30 %). All attempts to isolate pure samples of **4** failed.

Exchange reaction between 3 and two equivalents of $PhPH_2 \cdot BH_3$; synthesis of *meso-cis*-$[Pt(PPhH \cdot BH_3)_2(depe)]$ (5) and *rac-cis*-$[Pt(PPhH \cdot BH_3)_2(depe)]$ (6): A solution of $PhPH_2 \cdot BH_3$ (16 mg, 0.13 mmol) in CH_2Cl_2 (2 mL) was added to a solution of **3** (39 mg, 0.06 mmol) in CH_2Cl_2 (2 mL) at room temperature. After 22 h, the solvent was removed and the resulting oil was washed with toluene (5 mL) to remove $Ph_2PH \cdot BH_3$. The residue was dissolved in CH_2Cl_2/hexanes (1:1) and colorless, X-ray quality crystals of **5** were formed by slow evaporation at room temperature.

meso-cis-$[Pt(PPhH \cdot BH_3)_2(depe)]$ **5**: Yield was not determined; m.p. 184 – 185 °C; ^{1}H NMR (300 MHz, CD_2Cl_2): $\delta =$ 7.79 – 7.75 (m; Ph), 7.33 – 7.31 (m; Ph), 4.53 (br d, $^1J(H,P) = 328$ Hz; *J* PH), 2.28 – 2.20 (m; CH_2), 1.80 (br m, depe CH_2), 1.61 – 1.51 (m; CH_2), 1.18 (m; CH_3), 0.80 ppm (m; CH_3); $^{11}B\{^1H\}$ NMR (96 MHz, CD_2Cl_2): $\delta = -37.6$ ppm (br); $^{13}C\{^1H\}$ NMR (100 MHz, CD_2Cl_2): $\delta = 133.2$ (d, $^1J(C,P) = 40$ Hz, *ipso*-Ar), 135.5 (m; Ar), 129.6 (m; Ar), 128.3 (m; Ar), 24.5 (m; depe CH_2), 19.0 (m; CH_2), 9.2 ppm (m; CH_3); $^{31}P\{^1H\}$ NMR (121 MHz, CD_2Cl_2): $\delta = 58.5$ (m; $^2J(A,X') = {}^2J(A',X) = 230$ Hz, $^2J(A,X) = {}^2J(A',X') = -20$ Hz, $^2J(X,X') = 8$ Hz, $^2J(A,A') = 0$ Hz, $^1J(P,Pt) = 2099$ Hz; PEt_2), – 40.3 (br d, $^2J(P,P) = 241$ Hz, $^1J(P,Pt) = 1717$ Hz; PhPH); EI-MS (70 eV): *m*/*z* (%): 617 (4) $[(depe)Pt(PPh)_2]$, 541 (4) $[(depe)Pt(PPh)(PH)]$.

rac-cis-$[Pt(PPhH \cdot BH_3)_2(depe)]$ **6**: $^{31}P\{^1H\}$ NMR (121 MHz, CD_2Cl_2): $\delta = 57.6$ (m, $^2J(A,X') = {}^2J(A',X) = 230$ Hz, $^2J(A,X) = {}^2J(A',X') = -20$ Hz, $^2J(X,X') = 8$ Hz, $^2J(A,A') = 0$ Hz, $^1J(P,Pt) = 2119$ Hz; PEt_2), – 27.5 ppm (br d, $^2J(P,P) = 251$ Hz, $^1J(P,Pt) = 1678$ Hz; PhPH).

As **5** and **6** are stereoisomers, there was no difference found in the ^{1}H and ^{11}B NMR or EI-MS. Analysis for a mixture of **5** and **6** calcd (%) for $C_{22}H_{40}BP_4Pt$: C 40.83, H 6.54; found: C 40.89, H 6.61.

Reaction of $[Pt(depe)Cl_2]$ and $Li[PPhH \cdot BH_3]$: $Li[PPhH \cdot BH_3]$ was prepared by reacting a solution of $PhPH_2 \cdot BH_3$ (20 mg, 0.16 mmol) in THF (2 mL) with a solution of 1.6 M BuLi in hexanes (0.10 mL, 0.16 mmol) at 0 °C. The mixture was warmed to room temperature, and a solution of $[Pt(depe)Cl_2]$ (38 mg, 0.08 mmol) in THF (2 mL) was added. The mixture was stirred for 4 h, the volatiles were removed, and the residue was dissolved in CH_2Cl_2 and filtered to remove LiCl. The solution was shown by ^{31}P NMR to consist of an equal mixture of **5** and **6**.

Reaction of 1 and depe: A solution of depe (29 mg, 0.14 mmol) in THF (1 mL) was added to a solution of **1** (75 mg, 0.14 mmol) in THF (2 mL) at room temperature. The mixture was stirred for 1 h and the volatiles were removed in vacuo. The resulting oil showed a mixture of **5** and **6**. Similar results were obtained if C_6D_6 was used as a reaction solvent instead of THF.

Acknowledgements

This research was supported by the Petroleum Research Fund (PRF) administered by the American Chemical Society (ACS). C.A.J thanks the Ontario and Canadian governments for an Ontario Graduate Scholarship in Science and Technology (OGS-ST) (2001 – 2002) and a Natural Science and Engineering Research Council of Canada (NSERC) scholarship (2002 – 2004), H.D. thanks the Deutsche Forschungsgemeinschaft (DFG) for a postdoctoral fellowship and I.M thanks the Ontario government for a PREA award (1999 – 2004), the University of Toronto for a McLean Fellowship (1997 – 2003) and the Canadian government for a Canada Research Chair.

---

[1] C. T. Aitken, J. F. Harrod, E. Samuel, *J. Am. Chem. Soc.* **1986**, *108*, 4059.

[2] F. Gauvin, J. F. Harrod, H. G. Woo, *Adv. Organomet. Chem.* **1998**, *42*, 363.

[3] a) C. Aitken, J. F. Harrod, A. Malek, E. Samuel, *J. Organomet. Chem.* **1988**, *349*, 285; b) N. Choi, M. Tanaka, *J. Organomet. Chem.* **1998**, *564*, 81.

[4] For the formation of Ge–Ge bonds by means of Ru-catalyzed demethanative coupling, see: S. M. Katz, J. A. Reichl, D. H. Berry, *J. Am. Chem. Soc.* **1998**, *120*, 9844.

[5] a) T. Imori, T. D. Tilley, *J. Chem. Soc. Chem. Commun.* **1993**, 1607; b) T. Imori, V. Lu, H. Cai, T. D. Tilley, *J. Am. Chem. Soc.* **1995**, *117*, 9931; c) J. R. Babcock, L. R. Sita, *J. Am. Chem. Soc.* **1996**, *118*, 12481.

[6] a) N. Etkin, M. C. Fermin, D. W. Stephan, *J. Am. Chem. Soc.* **1997**, *119*, 2954; b) A. J. Hoskin, D. W. Stephan, *Angew. Chem.* **2001**, *113*, 1917; *Angew. Chem. Int. Ed.* **2001**, *40*, 1865; c) V. P. W. Böhm, M. Brookhart, *Angew. Chem.* **2001**, *113*, 4832; *Angew. Chem. Int. Ed.* **2001**, *40*, 4694.

[7] Q. Jiang, P. J. Carroll, D. H. Berry, *Organometallics* **1993**, *12*, 177.

[8] R. Shu, L. Hao, J. F. Harrod, H. G. Woo, E. Samuel, *J. Am. Chem. Soc.* **1998**, *120*, 12988.

[9] a) J. He, H. Q. Liu, J. F. Harrod, R. Hynes, *Organometallics*, **1994**, *13*, 336; b) H. Q. Liu, J. F. Harrod. *Organometallics*, **1992**, *11*, 822.

[10] L. J. Procopio, D. H. Berry, *J. Am. Chem. Soc.* **1991**, *113*, 4039.

[11] J. M. Fischer, W. E. Piers, S. D. Pearce Batchilder, M. J. Zaworotko, *J. Am. Chem. Soc.* **1996**, *118*, 283.

[12] a) Y. Li, Y. Kawakami, *Macromolecules* **1999**, *32*, 6871; b) R. Zhang, J. E. Mark, A. R. Pinhas, *Macromolecules* **2000**, *33*, 3508; c) T. E. Ready, B. P. S. Chauhan, P. Boudjouk, *Macromol. Rapid. Commun.* **2001**, *22*, 654.

[13] H. Dorn, R. A. Singh, J. A. Massey, A. J. Lough, I. Manners, *Angew. Chem.* **1999**, *111*, 3540; *Angew. Chem. Int. Ed.* **1999**, *38*, 3321.

[14] H. Dorn, R. A. Singh, J. A. Massey, J. M. Nelson, C. A. Jaska, A. J. Lough, I. Manners, *J. Am. Chem. Soc.* **2000**, *122*, 6669.

[15] For a recent extension to catalytic B–N bond formation, see: C. A. Jaska, K. Temple, A. J. Lough, I. Manners, *Chem. Commun.* **2001**, 962.

[16] H. Dorn, E. Vejzovic, A. J. Lough, I. Manners, *Inorg. Chem.* **2001**, *40*, 4327.

[17] E. Rivard, A. J. Lough, I. Manners, *J. Chem. Soc. Dalton Trans.* **2002**, 2966.

[18] a) L. Rosenberg, C. W. Davis, J. Yao, *J. Am. Chem. Soc.* **2001**, *123*, 5120; b) F.-G. Fontaine, D. Zargarian, *Organometallics* **2002**, *21*, 401.

[19] M. Okazaki, S. Ohshitanai, H. Tobita, H. Ogino, *Chem. Lett.* **2001**, 952.

[20] a) P. G. Pringle, M. B. Smith, *J. Chem. Soc. Chem. Commun.* **1990**, 1701; b) L.-B. Han, M. Tanaka, *J. Am. Chem. Soc.* **1996**, *118*, 1571; c) D. K. Wicht, I. V. Kourkine, B. M. Lew, J. M. Nthenge, D. S. Glueck, *J. Am. Chem. Soc.* **1997**, *119*, 5039; d) E. Costa, P. G. Pringle, K. Worboys, *Chem. Commun.* **1998**, 49.

[21] L.-B. Han, N. Choi, M. Tanaka, *Organometallics* **1996**, *15*, 3259.

[22] Other metals include Ru, Os, Nb, Ta and Ti. See, for example, ref. [23].

[23] For some recent reviews, see: a) H. Braunschweig, *Angew. Chem.* **1998**, *110*, 1882; *Angew. Chem. Int. Ed.* **1998**, *37*, 1786; b) G. J. Irvine, M. J. G. Lesley, T. B. Marder, N. C. Norman, C. R. Rice, E. G. Robins, W. R. Roper, G. R. Whittell, L. J. Wright, *Chem. Rev.* **1998**, *98*, 2685, and references therein.

[24] a) M. Shimoi, S. Ikubo, Y. Kawano, *J. Am. Chem. Soc.* **1998**, *120*, 4222; b) Y. Kawano, T. Yasue, M. Shimoi, *J. Am. Chem. Soc.* **1999**, *121*, 11744.

[25] a) C. N. Muhoro, X. He, J. F. Hartwig, *J. Am. Chem. Soc.* **1999**, *121*, 5033; b) S. Schlecht, J. F. Hartwig, *J. Am. Chem. Soc.* **2000**, *122*, 9435.

[26] a) M. Shimoi, S. Nagai, M. Ichikawa, Y. Kawano, K. Katoh, M. Uruichi, H. Ogino, *J. Am. Chem. Soc.* **1999**, *121*, 11704; b) T. Kakizawa, Y. Kawano, M. Shimoi, *Organometallics* **2001**, *20*, 3211.

[27] Preliminary communication: H. Dorn, C. A. Jaska, R. A. Singh, A. J. Lough, I. Manners, *Chem. Commun.* **2000**, 1041.

[28] W. Angerer, W. S. Sheldrick, W. Malisch, *Chem. Ber.* **1985**, *118*, 1261.

[29] A.-C. Gaumont, M. B. Hursthouse, S. J. Coles, J. M. Brown, *Chem. Commun.* **1999**, 63.

[30] D. A. Hoic, W. M. Davis, G. C. Fu, *J. Am. Chem. Soc.* **1996**, *118*, 8176.

[31] U. Vogel, M. Scheer, *Z. Anorg. Allg. Chem.* **2001**, *627*, 1593.

[32] For the recent synthesis of a phosphanylalane and phosphanylgallane complexes by means of a dehydrocoupling reaction involving a PH group of a coordinated PH_3 ligand, see: U. Vogel, A. Y. Timoshkin, M. Scheer, *Angew. Chem.* **2001**, *113*, 4541; *Angew. Chem. Int. Ed.* **2001**, *40*, 4409.

[33] S. Moreton, *Inorg. Chim. Acta.* **1994**, *215*, 67.

[34] D. K. Wicht, S. N. Paisner, B. M. Lew, D. S. Glueck, G. P. A. Yap, L. M. Liable-Sands, A. L. Rheingold, C. M. Haar, S. P. Nolan, *Organometallics* **1998**, *17*, 652.

[35] For example, the Tolman cone angles for the free phosphines $PhPH_2$ (101°) and Ph_2PH (128°) indicate that the primary phosphine has a smaller cone angle, C. A. Tolman, *Chem. Rev.* **1977**, *77*, 313. On the assumption that a BH_3 group would affect the cone angles in a systematic way, the smaller ligand should be the primary phosphidoborane.

[36] a) M. Baacke, S. Hietkamp, S. Morton, O. Stelzer, *Chem. Ber.* **1982**, *115*, 1389; b) A. J. Deeming, S. Doherty, J. E. Marshall, N. I. Powell; *J. Chem. Soc. Chem. Commun.* **1989**, 1351; c) A. J. Deeming, S. Doherty, *Polyhedron*, **1996**, *15*, 1175; d) A. J. Deeming, B. R. Cockerton, S. Doherty, *Polyhedron* **1997**, *16*, 1945.

[37] G. S. Hill, J. J. Vittal, R. J. Puddephatt, *Organometallics* **1997**, *16*, 1209.

[38] A related dehydrocoupling reaction involving a *dinuclear* palladium complex with a *bridging* hydride and Ph_2PH is known, see: M. A. Zhuravel, J. R. Moncarz, D. S. Glueck, K.-C. Lam, A. L. Rheingold, *Organometallics* **2000**, *19*, 3447.

[39] K. Bourumeau, A.-C. Gaumont, J.-M. Denis, *J. Organomet. Chem.* **1997**, *529*, 205.

[40] A. Sebald, B. Wrackmeyer, *J. Organomet. Chem.* **1986**, *304*, 271.

[41] T. Yoshida, T. Masuda, S. Otsuka, *Inorg. Synth.* **1979**, *19*, 110.

[42] Z. Otwinowski, W. Minor, *Methods Enzymol.* **1997**, *276*, 307.

[43] G. M. Sheldrick, SHELXTL-PC V5.1, Bruker Analytical X-Ray Systems Inc.: Madison, WI, **1997**.

[44] H. C. Clark, P. N. Kapoor, I. J. McMahon, *J. Organomet. Chem.* **1984**, *265*, 107.

Received: July 9, 2002 [F4236]